Comprehensive bioactivity of Pleurotus flabellatus lectin and their interruption in apoptosis inducing WNT pathway

Arul Kumar Murugesan (arulbot.kumar@gmail.com)
University of Madras
Malairaj Sathuvan
Shantou University
Anand Javee
University of Madras

Research Article

Keywords: Antifungal activity, Apoptosis, Colon cancer, DNA damage, Flow cytometry, Lung cancer

Posted Date: April 4th, 2022

DOI: https://doi.org/10.21203/rs.3.rs-1503491/v1

Abstract

Cancer is the high leading cause of cancer temporality worldwide. Treatment of cancer has always been a challenge for primary care and the development of appropriate medicine against colon and lung cancers is a major focus for budding researchers in the field. The mushroom lectin has, a few studies explored relating to the biological activity such as antibacterial, antifungal, anticancer activity and others. The mushroom lectin has attained considerable attention recently. The present study was undertaken to evaluate *Pleurotus flabellatus* lectin (PFL-L) induced cell death on human pathogenic fungal cells. Fungal cell viability was estimated at different intervals, moreover *Aspergillus niger* has the lowest cell viability (11%) compared to the others. Additionally, PFL-L was examined on human colorectal carcinoma cancer (HT29) cells and lung carcinoma cancer (A549) cells. The apoptotic changes were detected by apoptosis assay on HT29 cells and A549 cells. Further, PFL-L was demonstrated to the HT29 cells were disturbed against the presence of PFL-L at 100 µg/mL and the cell viability range is 25.90 ± 1.52%, whereas the A549 cells range is low. Then, the PFL-L initiates that DNA damage within cancer cells and the effects of cancer-related proteins were examined.

1. Introduction

In 2019, an reported around 1,335,100 new cancer patients distributed among 185 different countries from the world and 3,97,583 cancer-related deaths occurred among adolescents and young adults [1]. In 2030, the new and death causes are raised to doubling more cases to be increased [2]. Lung (11.7%), and colon (10.0%) cancer are the highest ratio when compared to other cancer. Colon cancer has now surpassed lung cancer as the leading incidence in 2020. Human lung cancer is the most unanimously diagnosed cancer and, closely followed by colorectal cancers [3]. The most treacherous cancers are arising from lung and colon organs from the human body. However many chemotherapy drugs represent the side effects of the immune system and arise different balance effects. The cancer death burden was disproportionately higher among women than men. The cancer death ratio varied substantially across, with the greater burden being in East Asia and South Asia [1]. Edible mushroom served as an antibacterial [4, 5], antifungal [6], antiviral [7], Anti-nociceptive and anti-inflammatory [8, 9], antioxidant [10] and anticancer [11] properties. Its beneficial potential act as different active bio-molecules including secondary metabolites [12]. Lectins are monomeric in nature and previously it's called hemagglutinins. The lectins or glycoproteins are widely present in animals [13], plants [14] virus [15], bacteria [16], fungi [17] and algae [18]. Lectins are traditionally extracted from the legume seeds and their vital function is recognized and binds reversibly to the carbohydrates as a binding protein [19]. Lectin bind to the carbohydrates in a reversibly recognized with highly specific mode and its structure to different variety of size and structure [20]. Lectin is clear evidence of a wide range for biotechnological and biomedical applications [21]. These lectins play the main role to control cancer cells as a tool of carbohydrate bind/recognition in different structural positions [22]. Many natural carbohydrate-binding proteins are participated to develop a new drug as a control/cure various diseases in a different manner [23, 24].

Many researchers take steps towards cancer-associated carbohydrate-binding proteins to alter tumor mechanisms. Specifically, MGL (Galactose-type Lectin) ligands from Chimeric MGL-Fc and mutant-MGL-Fc in colon cells [25]. This Galactose-type lectin is associated with colon cancer cells to alter the glycosylation process. The carbohydrate-binding proteins participate in early metastasis in various cancer cells [26]. Natural lectins have an enormous scientific interest to detect their biochemical functions in addition to biomedical applications. To recognize and interaction between cell and sugar moiety is most responsible for the inhibitory apoptosis mechanism. Fungal lectins have exhibited a high affinity to cancer and other related diseases and participate in very important functions within the inhibition of cellular proliferation with the initiation of early and late apoptosis processes [27]. Macro-fungi lectins are promising agents to control cancer cells. Since macro-fungi contain a large number of toxic glycoprotein/galectins involved as a defense mechanism against various parasites [28]. They have a symbiotic association between lectin and tumor cells. Fungal lectin can possibly control cancer through molecular mechanisms. Many pathways are described based on microRNAs and specific genes [29, 30]. Fungal glycoprotein to the cable induces a caspase-independent pathway in human cancer cells. The binding capacity of lectin and cancer cells through carbohydrate receptors [19]. Apoptosis cells can induce reactive oxygen species (ROS) in vast amounts during the mitochondrial process. Mechanistically, the ROS is a trigger to activate cancer expression proteins p53 and p38. Lectin can suppress p53 and p38 activity [31].

Our previous report has demonstrated that *P. flabellatus* lectin (PFL-L) displayed notable antibacterial activities toward several human pathogenic bacteria, such as *Bacillus subtilis, Staphylococcus aureus, Pseudomonas aeruginosa, Escherichia coli*, and *Klebsiella pneumonia*. Additionally, the PFL-L induced free radicals in the way of DPPH radical scavenging assay and Hydroxyl radical scavenging assay [32]. However, whether A549, and HT29 cells participated in PFL-L induced apoptosis to be investigated.

2. Materials And Methods

2.1 Material

3-(4,5- dimethylthiazol-2-yl)-2,5- diphenyltetrazolium bromide (MTT), 5 – fluroracil (5 – FU), 4’,6-diamidino-2-phenylinole (DAPI), Propidium Iodide (PI), Ethidium bromide (EB), RNase A (Ribonuclease A), EDTA, Phosphate-buffered Saline (PBS) pH 7.4, Dulbecco’s modified eagle medium (DMEM), Antibiotic solution, Fetal bovine serum (FBS), Trypsin 0.25% solution 1X, Dimethyl sulphoxide (DMSO), were purchased from Himedia Laboratories, Mumbai, India.

2.2. Assay of inhibitory activity of PFL-L on hyphal growth

Human pathogenic test fungus, *Aspergillus flavus* (AF017), *Mucor* sp (MC02). and *Aspergillus niger* (AN019) were obtained from Fungal Culture Collection Facility, CAS in Botany, University of Madras, Chennai, Tamil Nadu. Strains mature spore suspensions were grown on Potato Dextrose Broth (PDB) liquid medium at room temperature in a rotary shaker (200 rpm). Growth stage maintaining with proper subculture at fungal culture collection laboratory. After 7 days the strains were used as a further study.

The spore's suspension concentrations at 10^5 spores/ml of (80 µL) were added to a 96 well Microtiter plate [33].

The activities of PFL-L were determined against three different fungal strains using micro-dilution assays [34, 35]. PFL- L concentrations viz., 30 µg/ml, 40 µg/ml, 50 µg/ml, and 60 µg/ml of PFL-L were transferred to the Microtiter plate ($n = 3$). The media (PDB) were added to the all well and it gives final concentration at 120 µL. Standard drugs (70 µg/ml) were then added to the wells containing PDB suspension. The microtiter plates were maintained at an aseptic condition with tight tinfoil, sealed with parafilm, and incubated at 23–25ºC for 24 hours. Finally, the microtiter plates were measured at 570 nm by using a spectrophotometer (SpectraMaxM2^e, Multimode Plate Readers, California). To evaluate the IC_{50} value for the antifungal activity ten doses (10–100 µg/ml) of PFL-L and standard drug as per our previous report [36].

All measurements were conducted in triplicate. The percentage (%) of cell viability is calculated following formula,

$$\mathrm{Cellviability\%} = \frac{\mathrm{Absorbanceoftreatedcells}}{\mathrm{Absorbanceofcontrolcells}} \times 100$$

2.3. In-vitro anticancer activity

The HT29, A549 cancer cells, and fibroblast cell lines (3T3), were obtained from National Centre for Cell Science (NCCS), Pune, India. Cell lines were grown DMEM medium supplemented with FBS 10% (v/v) and Streptomycin with penicillin (250 U/mL) incubated 5% CO_2 incubator at 37˚C. The cells were allowed to grow for 24–48 hrs. The cell cultures were seeded in a 96 well plate, at a cell density of 1×10^5 cells/well and incubated for 24 h at 37˚C and 5% CO_2 [36, 37]. The cell viability and proliferation were evaluated after the cells get attached were treated against PFL-L (µg/ml) of different concentrations ranging from 10 to 100 µg/ml. After 24hr, the treated cells were washed with PBS (pH 7.4). Twenty microliters of MTT solution (5 mg/mL) were added to each well and allowed to stand for 4 h at 37˚C. Then, the medium with MTT was discarded and 100 µL of DMSO was added to each well to neutralize the dark blue formazan crystals. The microtiter plate was read a SpectraMaxM2^e, Multimode Plate Readers, California at 595nm. All the experiments were conducted in triplicates. The PFL-L inhibited at 50% of cell proliferation was observed as IC_{50} value. Morphology of all cell lines was observed using by bright field microscope.

The percentage (%) of cell viability are calculated following formula,

$$\mathrm{Cellviability\%} = \frac{\mathrm{Absorbanceoftreatedcells}}{\mathrm{Absorbanceofcontrolcells}} \times 100$$

2.4. Identification of apoptotic cells

To identify apoptotic cells, in presence of PFL-L treated cancer cells (HT29, A549) was examined by using a double staining method. The tested cells were washed with phosphate-buffered saline at pH 7.2 and fixed cells using, methanol: acetic acid 3:1 (v/v) for 10 min. After incubation, the tested cells were added in propidium iodide (PI), 50 µg/mL, and kept for 20 min to neutralize the reagents. Morphological analysis of the apoptotic cells was performed after staining with PI under a fluorescence microscope.

2.5. Determination of DNA damage by alkaline comet assay

The damage of the DNA was evaluated under alkaline conditions [38, 39]. The tested PFL-L and control cells were run the alkaline-based agarose gel with lysis buffer the following components, Tris – HCl (10 mM), pH 10, EDTA (100mM), sodium chloride (2.5M), DMSO (5%) and Triton X-100. HT29 and A549 cancer cells were embedded in low-melting-point agarose were lysed overnight at 4°C in lysis buffer. The unwinding step was performed by NaOH (300mM) and EDTA (1mM) for 40 min at 4°C (pH > 13). After running the gel, the slides were neutralized with Tris – HCl (0.4mM) pH at 7.5, and the cells were stained with ethidium bromide (2µg/ml). The DNA tail moment length was measured. The tail formation was scored by using a fluorescence microscope, Nikon, Japan.

2.6. Cell cycle analysis using flow cytometry method

To measure DNA ploidy as well as to measure alternations of cell cycle profiles characteristic of DNA fragmentation (necrosis) compared to patterned DNA cleavage (apoptosis). To determine the cell cycle analysis, 2.5×10^5 cells were incubated in 24 well plates with PFL-L in 0.5 ml of the medium at 5% CO_2 at 37˚C in the incubator [40]. After treatment, floating cells in the medium were pooled with attached cells collected by trypsinization. Cells were collected by centrifugation at 600g for 10 min at 4 ºC. Cells were washed with ice-cold PBS and fixed in 80% ethanol in PBS at – 20ºC. The fixed cells were pelleted and stained with PI (50 µg/mL) in the presence of RNase A (20 µg/mL) for 30 min at 37ºC. Apoptosis was quantitatively determined by flow cytometry after incubation at 4 ºC in the dark for at least 24 h cells containing nuclei with sub diploid DNA content. The number of cells at each stage of the cell was estimated by fluorescence-activated cell sorting (FACS) and monitored by flow cytometry. The data were analyzed to determine the percentage of cells at each phase of the cell cycle (G0/G1, S, and G2/M) or in the aneuploid peak.

2.7. Western blot analysis

To study the apoptosis nature of proteins on HT29 and A549 tested cells after 24 hours with PFL-L [41]. The equal amount of PFL-L was mixed with the sample buffer (2 X) and boiled for 5 minutes. The tested cell's protein was separated on SDS-PAGE (10%) and electro-transferred onto a PVDF membrane (Bio-Rad, USA). The blots were blocked with a blocking buffer (5%) for 4 hrs. After blocking, the membrane was incubated with respective rabbit monoclonal antibodies. Goat monoclonal antibody Bcl-Xl, Bcl-2, Procaspase-3, procaspase-9, MMP-3, MMP-9, B6, N-Cadherin, and E-Cadherin, in 1:5000 dilutions overnight at 4˚C. Then, the membranes were washed thrice with T-TBS for 10 minutes each, followed by horseradish peroxidase-conjugated secondary antibody (1:10,000 dilutions) and was incubated for 45

min at room temperature. Finally, signals were visualized using an enhanced chemiluminescent system (Pierce Biotechnology Inc, USA).

2.8. Statistical analysis

All experiments on both antifungal and anticancer activity tests were the average of triplicate analyses. The data were recorded as mean ± standard deviation.

3. Results And Discussion

3.1. PFL – L

The *Pleurotus flabellatus* (PFL-L) lectin was purified by using a DEAE – Cellulose anion exchange chromatography is followed by gel-filtration chromatography. The PFL–L chromatography is followed by gel-filtration chromatography. Arul Kumar et al (2021), previous findings indicates that the purity of PFL-L increased to 62.40% with the recovery of hemagglutinating activity by 12.12% [32].

3.2. Effect of PFL-L on fungal cell viability

Fungal cell viability was recorded on 1, 6, 12, 18, and 24 hours respectively. The *A. flavus, Mucor* sp. and *A. niger* spores were treated against PFL-L for different hours. *A. flavus* cell viability against PFL-L after four different time intervals was recorded. *A. flavus* treated with PFL-L and the cell viability range is 10% after 24 hours. While increased time, the cell viability was decreased due to the presence of PFL-L. The percentage of growth inhibition of *A. flavus* was reached in that dose-dependent manner (Fig. 1a). Table 1 indicates the IC_{50} value of *A. flavus* and range is 55.39 µg/ml. The standard drug (70mg/ml) was served as a control for the experiments at different time intervals. The *A. niger* showed low cell viability at 60 µg/ml after 24 hours of treatment of PFL-L. The *Mucor sp.* and *A. flavus* showed moderate activity against PFL-L at different incubation hours. *Mucor* sp activity was decreased on the highest concentration of PFL-L (60 µg/ml) after 24 hours incubation (Fig. 1b). The IC_{50} range of *Mucor* sp. is 110 µg/ml was recorded. After an hour of incubation of *A. niger* with 30 µg/ml of PFL-L, the inhibition percentage was zero, and the growth rate was found 100%. After 6 hours of inhibition, the growth rate of *A. niger* was minimized with an increase in the concentration of PFL-L. However, with the PFL-L concentrations at 60 µg/ml, the growth rate was reduced as a dependent by dose as well as time. After 6 hours, incubation with 60 µg/ml of PFL-L, the viability of *A. niger* cells was fully reduced and the mycelial cell viability reached 11%. PFL-L showed the highest activity in *A. niger* followed by *Mucor* sp. and *A. flavus* (Fig. 1c). PFL-L inhibited the 50% (IC_{50}), of hyphal growth of *A. niger, Mucor* sp. and *A. flavus* at 49.82 µg/ml, 55.39 µg/ml, and 110 µg/ml, respectively (Table 1). Recently, the researchers also reported that the fungal cell viability was more active against lectin from a mussel. The maximum level of inhibition of the fungal cells at 24h, and the original level recovered from 12h [33]. Similar to the previous result, PFL-L is shown to act as fungicidal properties. Lectin from leguminous plants (ConBr, DRL, and DvioL) have antifungal potential [42]. The lectin concentration of 100 µg/well has shown the lowest activity, compared with 200 µg/well of lectin against *A. niger* [43]. The PFL-L were similar results showed

that the carbohydrate-recognition protein C-type lectin from *Hemifusus pugilinus* (Hp-Lec) was against *A. niger* and *A. flavus* with 25 µg/ml and 50 µg/ml concentrations showed good mycelial inhibition after 25 hours intervals [44].

Table 1
Determination of Inhibitory Concentration (IC_{50}) against three human pathogenic fungi.

	A. niger	*A. flavus*	*Mucor* sp.
PFL (µg/ml)	49.82	55.39	110
Std.(µg/ml)	60.56	67.23	122.50
*All value is expressed as µg/ml from PFL-L.			

3.3. Cell proliferation assay

The effect of PFL-L on 3T3, HT29, and A549 was studied using an MTT assay. Among the different concentrations (20–100 µg/ml) of PFL-L has tested the different cancer cell lines. Figure 2a clearly indicated that the cell viability range is 10.27 ± 1.00% on A549 followed by HT29 was exhibited at 18.47 ± 1.53% with an effective inhibitory concentration of 60 µg/ml and 67 µg/ml. In the case of 3T3, upon treatment with different concentrations of (20–500 µg/ml), the viability of cells reduced at 48.60 ± 1.17% with an inhibitory concentration of 86.68 µg/ml. The IC_{50} ranges were observed on A549, and HT29, which are 60 µg/ml, and 67µg/ml respectively. From cell proliferation assay to confirm PFL-L against colon and lung cancer cells were more potential cytotoxicity. The 3T3 cell line showed 50% inhibition at 486.68 µg/ml (Fig. 2b). Even at the concentration of 100 µg/ml of PFL-L, 89% of cell viability was observed without any cell growth arrest/disturbance which confirmed that PFL-L does not have any toxic effect on normal human cell lines. There was no wide range of morphological changes were observed in normal fibroblast cell lines upon treatment with PFL-L. In the case of different cancer cell lines, in the lead treatment of PFL-L, morphological changes were observed by shrinkage, round-shaped, and damaging the cell membrane (Fig. 3).

Condensation of nuclear chromatin was also observed after 24hrs of incubation. *Bauhinia ungulata* demonstrated the cytotoxicity assay against HT-29 cell line of human colon adenocarcinoma similar to dose-dependent manner on PFL-L [45]. Lectin (LCL) from *Lantana camara* induced HT29 growth based on time and dose-dependent manner [46]. Madhu et al reported chitin-specific lectin from *Praecitrullus fistulosus* was strong cytotoxicity against colon cancer at 500 mg/ml [47]. Lung carcinoma (A549) cells showed the highest growth of inhibition at low-level dose concentration on PFL-L than others. In contrast, HT29 was the highest activity compared with A549 cells. Whereas, the Galactose-type Lectin (MGL) showed strong anticancer activity against colon cancer cell lines [25]. While on the contrary, on lung cancer against Daboialectin (C-type) from Russells viper venom-induced cell cytoskeletal damage on lung cancer cells [48].

3.4. Identification of apoptotic cells

Nuclear staining assay consistently showed control and treated cancer cells against PFL-L. Cell death has occurred on A549 and HT29 in presence of PFL-L. Morphological changes were analyzed by acridine orange/ethidium bromide (AO/EB) and DAPI staining. In the treatment of AO/ EB staining were indicated green color for live cells, orange color indicates early apoptotic cells; red color indicates late apoptotic dead cells. The dark blue color was indicated in the DAPI stain. EB stain enters into the cell when loss of membrane integrity. AO and EB were binding on the nucleus of dead cells and necrotic cells. HT29 cells were treated with IC_{50} the range is 67µg/ml after 24 hours. The presence of PFL-L on HT29 cells were dead condition was shown in Fig. 4a. AO was bound with both live cells and dead cells. In contrast, Fig. 4b was indicating, A549 cells treated with PFL-L at 60 µg/ml showed green color. The absence of PFL-L showed no dead cells. Morphological changes on A549 occurred at 60 µg/ml in dark green color with AO. EB stained were negligible within cells in the condition of without PFL-L. The presence of PFL-L at IC_{50} on A549 found apoptotic cells. Absences of PFL-L in AO, EB, AO/EB, and DAPI no necrotic or apoptotic cells were found. Cell death is categorized by two divisions based on cell death viz., necrosis, and apoptosis. The necrosis was showed accidental cell death and their morphology lose/lysis membrane structure. Due to condensation of nucleus chromatin were indicated red cells. Apoptosis was indicates programmed cell death and the cell membrane structure goes too small in size / bound vesicles. [49]. In A549 and HT29 cells, membrane integrity, nuclear shrinkage/segmentation, and condensation of chromatin were observed after 24hours upon treatment of PFL-L. Morphological evidence showed lectin-induced apoptosis in colorectal adenocarcinoma cells and lung carcinoma cells. Apoptosis on cancer cells was reported by [50]. A549 cells were treated with 60 µg/ml of marine-derived lectin-induced degeneration cytoplasmic material, it is strong evidence for PFL-L induced apoptosis [51]. *Kaempferia rotunda* lectin (KRL) inhibited the proliferation of colon cancer cells at the doses of 0.25, 0.5, and 1.0 mg/ml, respectively [52]. C-type lectin from Russell's viper venom and *Polygonatum odoratum* lectin (POL) induced apoptosis in human lung cancer cells in Daboialectin (50 and 100 nM) and POL with 23 µg/ml for 24 h and 48 h, respectively [29, 48].

3.5. Comet assay

The PFL-L was treated with A549 (60 µg/mL) and HT29 (67 µg/ml) cells for 24 hours. The DNA fragmentation was evaluated as shown in Fig. 5. The IC_{50} range was induced tail formation on A549 and HT29 cells. In addition, the presence of PFL-L showed maximum tail movement on A549 cells (13.13 ± 2.80) followed by HT29 cells (13.09 ± 1.31) respectively (Table 2). In contrast, the absence of PFL-L tail in A549 cells and HT29 cells were observed 3.68 ± 1.04, 0.36 ± 0.45 respectively. Therefore, PFL-L can induce A549 and HT29 cells apoptosis. The early apoptosis was indicating DNA damage (tail formation) by the alkaline nature of single gel electrophoresis. The single cells of DNA strand breaks/damage were detected apoptosis changes. [53, 54]. The comet/ single cell gel electrophoresis strongly indicated DNA damage and apoptosis in A549 and HT29 cells. ACL induced DNA fragmentation from *Allium chinense* with 100 µg/ml [55].

Table 2

DNA head and tail calculated for absence/presence of PFL-L. DNA tail movement was measured from eight different single cells (n = 8). DNA tail formation of single cells from A549 and HT29 cells in presence of IC_{50} values.

		Head	Tail
A549	Control	96.31 ± 1.04	3.68 ± 1.04
	Treated	86.87 ± 1.52	13.13 ± 2.80
HT29	Control	99.63 ± 0.45	0.36 ± 0.45
	Treated	87.03 ± 1.52	13.09 ± 1.31

* The experiments were calculated standard deviation from n = 8 (Mean ± SD; n = 8).

3.6. Cell cycle analysis

Cell cycle analysis was evaluated for both control and treated A549 and HT29 cell lines by flow cytometry. The presence/absence of PFL-L at IC_{50} concentration was treated on A549 cells and HT29 cells were studied. Figure 6a,d showed the absence of PFL-L on HT29 cell cycle phase indicate (≥ 30%). Interestingly, the SubG0 phase cell population increased (≤ 40%) after 24 hours of incubation with 67 µg/ml of PFL-L. However, after 24 hours, HT29 cell's apoptotic range decreased at the G0G1 phase (≤ 30%). HT29 cells population arrest at SubG0 phase undergoes apoptosis in presence of PFL-L (Table 3). The apoptotic range was identified at the G0G1 phase in HT29 cell's. S phase and G2M phase gradually decrease cell population in the absence of PFL-L on HT29 cells (Fig. 6b). PFL-L induced apoptosis on HT29 cells. A549 cells are significantly similar to HT29 cells. After 24 hours of incubation, A549 cells were arrested at the subG0 phase. A549 cells on the absence of PFL-L cell population range below 20% while, presence of PFL-L range was above 60% (Fig. 6d) respectively. Interestingly, the G0G1 phase increase (≤ 60%) in absence of PFL-L, but PFL-L at 60 µl/mg reduces cell population percentage (≥ 40%). In contrast, the presence of PFL-L induces apoptosis on A549 cells (Fig. 6e,f). Cell cycle analysis was measured by Flow cytometry to determine apoptotic cell arrest point. Forward-scattered light (FSC) and Side-scattered (SCC) light with fluorescence light (FL) correlate the cell cycle phase in FACS Calibur. The scatter light beam exposed on cells showed cell death, cell membrane breakage, condensation of chromatin, fragmentation of DNA materials, shrinkage of cells, and apoptosis cells [56]. Mannose-binding lectin (MBL) from *Oreochromis niloticus* was induced apoptosis at 50 µg/mL [57]. The macrophage Galactose-type Lectin (MGL2) arrest on lung tumor cells in the nature of Tn antigen. The carbohydrate recognizing domain such as CRD fused with MGL2 immuno-suppression conforming by a lectin-dependent mechanism [58].

Table 3

Percentages of cells each phase absence or presence of PFL-L. Apoptosis were identified at G0G1 phase with absence or/ presence of PFL-L on HT29 and A549 cells after 24 hours.

	A549 cells (%)		HT29 cells (%)	
	Control	Treated	Control	Treated
Sub Go	4.87 ± 1.35	55.46 ± 0.66	21.91 ± 1.72	43.70 ± 1.87
GoG_1	62.41 ± 3.55	31.29 ± 1.03	43.57 ± 1.57	29.43 ± 2.95
S	17.82 ± 1.51	6.93 ± 0.82	16.42 ± 3.54	13.76 ± 3.10
G_2M	14.55 ± 3.48	5.21 ± 2.11	14.65 ± 5.90	10.94 ± 3.73
* The cell cycle phase analyzed at three time interval (n = 3).				
Standard deviation calculated from n = 3 cell cycle analysis by flow cytometry (Mean ± SD; n = 3).				

3.7. Effects of PFL-L on the expression of apoptotic regulatory proteins

In order to study the effect of PFL-L on apoptosis regulatory proteins were examined on A549 cells. Figure 7a shows the apoptosis-related protein in Bax/Bcl2 range was recorded based on the down-regulation process. The disruption of the mitochondrial plasma membrane by PFL-L activated the proteins by cleaving pro-caspases3 and 9 and target protein PARP, respectively. In contrast that PFL-L could induce apoptosis through the regulation of apoptosis-related protein expression in A549 cells. From the results, PFL-L-induced apoptosis was demonstrated. The treatment of A549 cells has markedly elevated the presence of PFL-L after 24 hours. The apoptosis-related protein inhibitory ratio in a dose-dependent manner [59]. Mitochondrial-related protein was regulated to the caspase-dependent mechanism [60]. From the above study were supported to the PFL-L was to inhibit mitochondria pore at the time apoptosis mechanism. Next, we explored the HT20 cells treated with PFL-L after 24 hours. The Fig. 7b results showed that PFL-L significantly reduced the proteins levels of MMP-3, MMP-9, B6, N-cadherin, and E-cadherin. From our results, the MMP protein which is a downstream process and protein behaviors on HT29 cells were changed. Cheng Peng et al (2016), were reported the mesenchymal-epithelial transition (MET) process regulating the epithelial-mesenchymal transition (EMT) and its important role to play on colon cancer cells [61]. EMT process was interrupted the WNT pathway. After PFL-L was treated with HT29 cells for 24 hours, we detected the MMP and cadherin protein levels were decreased. The expression of colon cancer-related proteins such as N-cadherin and E-cadherin were up-regulated. MMP was involving, many signaling pathways by transcriptions process [62]. The mitochondrial-related proteins such as Bcl-2 and its act pro-apoptotic protein in colon cancer. Bcl-2 family interacting with a mitochondrial-associated pathway [63]. From our results, the control Bcl-2 and Bcl-xL were stimuli for the pro-apoptotic members.

Conclusions

Conclusion

Present scenario, touching the most common cancer metastatic stages has high and the survival rate is low. However, the chemotherapy against different cancer treatments and control measured to provide limited success causes with more side effects. Moreover, cancer drug developments with non-toxic drugs are manipulated from natural sources. The fungal lectin is emphasized to the urgent need to implement the natural carbohydrate-binding protein towards cancer cells metastatic stages control. In summary, we conclude that the induction of the cancer-related caspase-dependent activity of Bax/Bcl2, and MMP/cadherin proteins may be involved in the cytotoxicity of PFL-L in HT29 and A549 cells. Our investigation has proved that *Pleurotus flabellatus* lectin can be a promising candidate for treating human colon and lung cancer.

Declarations

Authors' contributions

Arul Kumar Murugesan; Conceptualization, Validation, Formal Analysis, Investigation, Methodology, Resources, Writing - Review & Editing. **Malairaj Sathuvan;** Investigation, Methodology, Resources, Writing - Review & Editing. Data curation**. Anand Javee ;** Investigation, Methodology, Resources, Writing - Review & Editing. Data curation**.**

Conflicts of interest

The authors declare that they have no known competing financial interests or personal relationships that could have appeared to influence the work reported here.

Ethical approval:

This article does not contain any studies with animals performed by any of the authors.

Funding

The authors declare that no funds, grants, or other support were received during the preparation of this manuscript.

Consent to participate and for publication

Informed consent was obtained from all individual participants included in the study.

Availability of Data and Materials

The data that support the findings of this study are available from the corresponding author, (AKM), on special request.

Acknowledgement

Authors thankful to Late **Prof. J. Muthumary, D.Sc.,** Mentor, CAS in Botany for invaluable guidance, constant support and encouragement, constructive criticism of my research work. The authors thankful to **the Director, Centre for Advanced Studies in Botany, University of Madras**, Chennai, India for providing facilities. The author also thank the **Head of the Department, Department of Botany, Bharathidasan University**, Tiruchirappalli- 620 024, Tamil Nadu, India; for providing constant support.

References

1. L. You, Z. Lv, C. Li, W. Ye, Y. Zhou, J. Jin, Q. Han, Worldwide cancer statistics of adolescents and young adults in 2019: a systematic analysis of the Global Burden of Disease Study 2019, ESMO Open. 6 (2021) 1–13. https://doi.org/10.1016/j.esmoop.2021.100255.
2. F. Bray, J. Ferlay, I. Soerjomataram, R.L. Siegel, L.A. Torre, A. Jemal, Global cancer statistics 2018: GLOBOCAN estimates of incidence and mortality worldwide for 36 cancers in 185 countries, CA. Cancer J. Clin. 68 (2018) 394–424. https://doi.org/10.3322/caac.21492.
3. H. Sung, J. Ferlay, R.L. Siegel, M. Laversanne, I. Soerjomataram, A. Jemal, F. Bray, Global Cancer Statistics 2020: GLOBOCAN Estimates of Incidence and Mortality Worldwide for 36 Cancers in 185 Countries, CA. Cancer J. Clin. 71 (2021) 209–249. https://doi.org/10.3322/caac.21660.
4. M.I. Petrova, E. Lievens, T.L.A. Verhoeven, J.M. MacKlaim, G. Gloor, D. Schols, J. Vanderleyden, G. Reid, S. Lebeer, The lectin-like protein 1 in Lactobacillus rhamnosus GR-1 mediates tissue-specific adherence to vaginal epithelium and inhibits urogenital pathogens, Sci. Rep. 6 (2016) 1–15. https://doi.org/10.1038/srep37437.
5. P.M. da Silva, M.C. de Moura, F.S. Gomes, D. da Silva Trentin, A.P. Silva de Oliveira, G.S.V. de Mello, M.G. da Rocha Pitta, M.J.B. de Melo Rego, L.C.B.B. Coelho, A.J. Macedo, R.C.B.Q. de Figueiredo, P.M.G. Paiva, T.H. Napoleão, PgTeL, the lectin found in Punica granatum juice, is an antifungal agent against Candida albicans and Candida krusei, Int. J. Biol. Macromol. 108 (2018) 391–400. https://doi.org/10.1016/j.ijbiomac.2017.12.039.
6. E.A. Speakman, I.M. Dambuza, F. Salazar, G.D. Brown, T Cell Antifungal Immunity and the Role of C-Type Lectin Receptors, Trends Immunol. 41 (2020) 61–76. https://doi.org/10.1016/j.it.2019.11.007.
7. K. Młynarczyk, D. Walkowiak-Tomczak, G.P. Łysiak, Bioactive properties of Sambucus nigra L. As a functional ingredient for food and pharmaceutical industry, J. Funct. Foods. 40 (2018) 377–390. https://doi.org/10.1016/j.jff.2017.11.025.
8. B.O. Oladokun, O.N. Omisore, O.A. Osukoya, A. Kuku, Anti-nociceptive and anti-inflammatory activities of Tetracarpidium conophorum seed lectin, Sci. African. 3 (2019). https://doi.org/10.1016/j.sciaf.2019.e00073.
9. T.P.C. Fontenelle, G.C. Lima, J.X. Mesquita, J.L. de S. Lopes, T.V. de Brito, F. das C. Vieira Júnior, A.B. Sales, K.S. Aragão, M.H.L.P. Souza, A.L. dos R. Barbosa, A.L.P. Freitas, Lectin obtained from the red seaweed Bryothamnion triquetrum: Secondary structure and anti-inflammatory activity in mice, Int. J. Biol. Macromol. 112 (2018) 1122–1130. https://doi.org/10.1016/j.ijbiomac.2018.02.058.

10. M. Wu, C. Tong, Y. Wu, S. Liu, W. Li, A novel thyroglobulin-binding lectin from the brown alga Hizikia fusiformis and its antioxidant activities, Food Chem. 201 (2016) 7–13. https://doi.org/10.1016/j.foodchem.2016.01.061.
11. S.K. Bhutia, P.K. Panda, N. Sinha, P.P. Praharaj, C.S. Bhol, D.P. Panigrahi, K.K. Mahapatra, S. Saha, S. Patra, S.R. Mishra, B.P. Behera, S. Patil, T.K. Maiti, Plant lectins in cancer therapeutics: Targeting apoptosis and autophagy-dependent cell death, Pharmacol. Res. 144 (2019) 8–18. https://doi.org/10.1016/j.phrs.2019.04.001.
12. I. Hasan, Y. Ozeki, Y. Ozeki, Accepted Manuscript, (2018).
13. X. Yin, L. Mu, Y. Li, L. Wu, Y. Yang, X. Bian, B. Li, S. Liao, Y. Miao, J. Ye, S. Immunology, Accepted Manuscript, (2018).
14. A.C. Ribeiro, R. Ferreira, R. Freitas, Plant Lectins: Bioactivities and Bioapplications, 2018. https://doi.org/10.1016/B978-0-444-64056-7.00001-5.
15. A.J. Thompson, L. Cao, Y. Ma, X. Wang, J.K. Diedrich, C. Kikuchi, S. Willis, C. Worth, R. McBride, J.R. Yates, J.C. Paulson, Human Influenza Virus Hemagglutinins Contain Conserved Oligomannose N-Linked Glycans Allowing Potent Neutralization by Lectins., Cell Host Microbe. (2020) 1–11. https://doi.org/10.1016/j.chom.2020.03.009.
16. P. Sýkorová, J. Novotná, G. Demo, G. Pompidor, E. Dubská, J. Komárek, E. Fujdiarová, J. Houser, L. Hároníková, A. Varrot, N. Shilova, A. Imberty, N. Bovin, M. Pokorná, M. Wimmerová, Characterization of novel lectins from Burkholderia pseudomallei and Chromobacterium violaceum with seven-bladed β-propeller fold, Int. J. Biol. Macromol. (2019). https://doi.org/10.1016/j.ijbiomac.2019.10.200.
17. R.S. Singh, A.K. Walia, J.F. Kennedy, Journal Pre-proofs, (2019).
18. T. Lafarga, F.G. Acién-Fernández, M. Garcia-Vaquero, Bioactive peptides and carbohydrates from seaweed for food applications: Natural occurrence, isolation, purification, and identification, Algal Res. 48 (2020). https://doi.org/10.1016/j.algal.2020.101909.
19. A.K. Gautam, D. Sharma, J. Sharma, K.C. Saini, D. Sharma, J. Sharma, K.C. Saini, Journal Pre-proofs, (2019).
20. L.C.B.B. Coelho, P.M.D.S. Silva, V.L.D.M. Lima, E.V. Pontual, P.M.G. Paiva, T.H. Napoleão, M.T.D.S. Correia, Lectins, Interconnecting Proteins with Biotechnological/Pharmacological and Therapeutic Applications, Evidence-Based Complement. Altern. Med. 2017 (2017). https://doi.org/10.1155/2017/1594074.
21. A.J. Pietrzyk-Brzezinska, A. Bujacz, H-type lectins – Structural characteristics and their applications in diagnostics, analytics and drug delivery, Int. J. Biol. Macromol. 152 (2020) 735–747. https://doi.org/10.1016/j.ijbiomac.2020.02.320.
22. R. Cagliari, F.S. Kremer, L. da S. Pinto, Bauhinia lectins: Biochemical properties and biotechnological applications, Int. J. Biol. Macromol. 119 (2018) 811–820. https://doi.org/10.1016/j.ijbiomac.2018.07.156.
23. A.M. Oommen, N. Somaiya, J. Vijayan, S. Kumar, S. Venkatachalam, L. Joshi, GlycoGAIT: A web database to browse glycogenes and lectins under gastric inflammatory diseases, J. Theor. Biol. 406

(2016) 93–98. https://doi.org/10.1016/j.jtbi.2016.07.020.

24. C. Apfelthaler, P. Gassenbauer, S. Weisse, F. Gabor, M. Wirth, A lectin mediated delivery system for the intravesical treatment of bladder diseases using poly-(L)-glutamic acid as polymeric backbone, Eur. J. Pharm. Sci. 111 (2018) 376–382. https://doi.org/10.1016/j.ejps.2017.10.011.
25. M. Pirro, Y. Rombouts, A. Stella, O. Neyrolles, O. Burlet-Schiltz, S.J. van Vliet, A.H. de Ru, Y. Mohammed, M. Wuhrer, P.A. van Veelen, P.J. Hensbergen, Characterization of Macrophage Galactose-type Lectin (MGL) ligands in colorectal cancer cell lines, Biochim. Biophys. Acta - Gen. Subj. 1864 (2020). https://doi.org/10.1016/j.bbagen.2020.129513.
26. C. Fu, H. Zhao, Y. Wang, H. Cai, Y. Xiao, Y. Zeng, H. Chen, Tumor-associated antigens: Tn antigen, sTn antigen, and T antigen, Hla. 88 (2016) 275–286. https://doi.org/10.1111/tan.12900.
27. E. Nutku, H. Aizawa, S.A. Hudson, B.S. Bochner, Ligation of Siglec-8: A selective mechanism for induction of human eosinophil apoptosis, Blood. 101 (2003) 5014–5020. https://doi.org/10.1182/blood-2002-10-3058.
28. V. Trigueros, A. Lougarre, D. Ali-Ahmed, Y. Rahbé, J. Guillot, L. Chavant, D. Fournier, L. Paquereau, Xerocomus chrysenteron lectin: Identification of a new pesticidal protein, Biochim. Biophys. Acta - Gen. Subj. 1621 (2003) 292–298. https://doi.org/10.1016/S0304-4165(03)00098-9.
29. L. Wu, T. Liu, Y. Xiao, X. Li, Y. Zhu, Y. Zhao, J. Bao, C. Wu, Polygonatum odoratum lectin induces apoptosis and autophagy by regulation of microRNA-1290 and microRNA-15a-3p in human lung adenocarcinoma A549 cells, Int. J. Biol. Macromol. 85 (2016) 217–226. https://doi.org/10.1016/j.ijbiomac.2015.11.014.
30. B. Liu, J.M. Wu, J. Li, J.J. Liu, W.W. Li, C.Y. Li, H.L. Xu, J.K. Bao, Polygonatum cyrtonema lectin induces murine fibrosarcoma L929 cell apoptosis and autophagy via blocking Ras-Raf and PI3K-Akt signaling pathways, Enferm. Infecc. Microbiol. Clin. 28 (2010) 1934–1938. https://doi.org/10.1016/j.biochi.2010.08.009.
31. B. Liu, Y. Cheng, B. Zhang, H. jiao Bian, J. ku Bao, Polygonatum cyrtonema lectin induces apoptosis and autophagy in human melanoma A375 cells through a mitochondria-mediated ROS-p38-p53 pathway, Cancer Lett. 275 (2009) 54–60. https://doi.org/10.1016/j.canlet.2008.09.042.
32. A.K. Murugesan, K.S. Gunasagaran, Purification and characterization of a synergistic bioactive lectin from Pleurotus flabellatus (PFL-L) with potent antibacterial and in-vitro radical scavenging activity, Anal. Biochem. 635 (2021) 114450. https://doi.org/10.1016/j.ab.2021.114450.
33. I. V. Chikalovets, O. V. Chernikov, M. V. Pivkin, V.I. Molchanova, A.P. Litovchenko, W. Li, P.A. Lukyanov, A lectin with antifungal activity from the mussel crenomytilus grayanus, Fish Shellfish Immunol. 42 (2015) 503–507. https://doi.org/10.1016/j.fsi.2014.11.036.
34. A.M. Troskie, N.M. Vlok, M. Rautenbach, A novel 96-well gel-based assay for determining antifungal activity against filamentous fungi, J. Microbiol. Methods. 91 (2012) 551–558. https://doi.org/10.1016/j.mimet.2012.09.025.
35. E.A. Du Toit, M. Rautenbach, A sensitive standardised micro-gel well diffusion assay for the determination of antimicrobial activity, J. Microbiol. Methods. 42 (2000) 159–165.

https://doi.org/10.1016/S0167-7012(00)00184-6.

36. A.K. Murugesan, B. Pannerselvam, A. Javee, M. Rajenderan, D. Thiyagarajan, Facile green synthesis and characterization of Gloriosa superba L. tuber extract-capped silver nanoparticles (GST-AgNPs) and its potential antibacterial and anticancer activities against A549 human cancer cells, Environ. Nanotechnology, Monit. Manag. 15 (2021) 100460. https://doi.org/10.1016/j.enmm.2021.100460.
37. T. Mosmann, Rapid colorimetric assay for cellular growth and survival: Application to proliferation and cytotoxicity assays, J. Immunol. Methods. 65 (1983) 55–63. https://doi.org/10.1016/0022-1759(83)90303-4.
38. P.L. Olive, J.P. Banáth, The comet assay: A method to measure DNA damage in individual cells, Nat. Protoc. 1 (2006) 23–29. https://doi.org/10.1038/nprot.2006.5.
39. N.P. Singh, M.T. McCoy, R.R. Tice, E.L. Schneider, A simple technique for quantitation of low levels of DNA damage in individual cells, Exp. Cell Res. 175 (1988) 184–191. https://doi.org/10.1016/0014-4827(88)90265-0.
40. P. Pozarowski, Z. Darzynkiewicz, Analysis of cell cycle by flow cytometry., Methods Mol. Biol. 281 (2004) 301–311. https://doi.org/10.1385/1-59259-811-0:301.
41. T. Suzuki, H. Park, E. Anderson Till, W.J. Lennarz, The PUB domain: A putative protein-protein interaction domain implicated in the ubiquitin-proteasome pathway, Biochem. Biophys. Res. Commun. 287 (2001) 1083–1087. https://doi.org/10.1006/bbrc.2001.5688.
42. B.S. Gomes, A.B.S. Siqueira, R. de C.C. Maia, V. Giampaoli, E.H. Teixeira, F.V.S. Arruda, K.S. do Nascimento, A.N. de Lima, C.M. Souza-Motta, B.S. Cavada, A.L.F. Porto, Antifungal activity of lectins against yeast of vaginal secretion, Brazilian J. Microbiol. 43 (2012) 770–778. https://doi.org/10.1590/S1517-83822012000200042.
43. Q. Yan, Z. Jiang, S. Yang, W. Deng, L. Han, A novel homodimeric lectin from Astragalus mongholicus with antifungal activity, Arch. Biochem. Biophys. 442 (2005) 72–81. https://doi.org/10.1016/j.abb.2005.07.019.
44. J. Sivakamavalli, K. Park, I.S. Kwak, B. Vaseeharan, Purification and partial characterization of carbohydrate-recognition protein C-type lectin from Hemifusus pugilinus, Carbohydr. Res. 499 (2021). https://doi.org/10.1016/j.carres.2020.108224.
45. H.C. Silva, L.D.S. Pinto, E.H. Teixeira, K.S. Nascimento, B.S. Cavada, A.L.C. Silva, BUL: A novel lectin from Bauhinia ungulata L. seeds with fungistatic and antiproliferative activities, Process Biochem. 49 (2014) 203–209. https://doi.org/10.1016/j.procbio.2013.10.020.
46. R. Ransing, F. Adiukwu, V. Pereira-sanchez, R. Ramalho, L. Orsolini, M. Pinto, J. Soler-vidal, Journal Pre-proof, (2020). https://doi.org/10.1016/j.ajp.2020.102085.
47. C.S. Madhu, K.S. Balaji, J. Shankar, A.C. Sharada, Antitumor effects of chitin specific lectin from Praecitrullus fistulosus by targeting angiogenesis and apoptosis, Biochem. Biophys. Res. Commun. 518 (2019) 381–387. https://doi.org/10.1016/j.bbrc.2019.08.067.
48. J. Pathan, S. Mondal, A. Sarkar, D. Chakrabarty, Daboialectin, a C-type lectin from Russell's viper venom induces cytoskeletal damage and apoptosis in human lung cancer cells in vitro, Toxicon. 127

(2017) 11–21. https://doi.org/10.1016/j.toxicon.2016.12.013.

49. I. Vermes, C. Haanen, Apoptosis and programmed cell death in health and disease, Adv. Clin. Chem. 31 (1994) 177–246. https://doi.org/10.1016/S0065-2423(08)60336-4.
50. Y.P. Bhandary, S.K. Shetty, A.S. Marudamuthu, R. Margaret, S. Idell, M. Gharaee-kermani, R.S. Shetty, B.C. Starcher, Y.P. Bhandary, S.K. Shetty, A.S. Marudamuthu, M.R. Gyetko, S. Idell, M. Gharaee-kermani, R.S. Shetty, B.C. Starcher, S. Shetty, Regulation of alveolar epithelial cell apoptosis and pulmonary fibrosis by coordinate expression of components of the fibrinolytic system Regulation of alveolar epithelial cell apoptosis and pulmonary fibrosis by coordinate expression of components of the, (2013). https://doi.org/10.1152/ajplung.00099.2011.
51. W.K. Wang, Q.H. Lu, J.N. Zhang, B. Wang, X.J. Liu, F.S. An, W.D. Qin, X.Y. Chen, W.Q. Dong, C. Zhang, Y. Zhang, M.X. Zhang, HMGB1 mediates hyperglycaemia-induced cardiomyocyte apoptosis via ERK/Ets-1 signalling pathway, J. Cell. Mol. Med. 18 (2014) 2311–2320. https://doi.org/10.1111/jcmm.12399.
52. F. Islam, V. Gopalan, A.K.Y. Lam, S.R. Kabir, Kaempferia rotunda tuberous rhizome lectin induces apoptosis and growth inhibition of colon cancer cells in vitro, Int. J. Biol. Macromol. 141 (2019) 775–782. https://doi.org/10.1016/j.ijbiomac.2019.09.051.
53. Y. Lu, Y. Liu, C. Yang, Evaluating in vitro DNA damage using comet assay, J. Vis. Exp. 2017 (2017) 2–7. https://doi.org/10.3791/56450.
54. S. Nandhakumar, S. Parasuraman, M.M. Shanmugam, K. Ramachandra Rao, P. Chand, B. Vishnu Bhat, Evaluation of DNA damage using single-cell gel electrophoresis (Comet Assay), J. Pharmacol. Pharmacother. 2 (2011) 107–111. https://doi.org/10.4103/0976-500X.81903.
55. X. Xiao, H. He, X. Ding, Q. Yang, X. Liu, S. Liu, J. Rang, T. Wang, M. Zuo, L. Xia, Purification and cloning of lectin that induce cell apoptosis from Allium chinense, Phytomedicine. 22 (2015) 238–244. https://doi.org/10.1016/j.phymed.2014.12.004.
56. Z. Darzynkiewicz, X. Huang, M. Okafuji, M.A. King, Cytometric methods to detect apoptosis, Methods Cell Biol. 2004 (2004) 307–341. https://doi.org/10.1016/s0091-679x(04)75012-8.
57. L. Mu, X. Yin, Y. Yang, L. Wu, H. Wu, B. Li, Z. Guo, J. Ye, Functional characterization of a mannose-binding lectin (MBL) from Nile tilapia (Oreochromis niloticus) in non-specific cell immunity and apoptosis in monocytes/macrophages, Fish Shellfish Immunol. 87 (2019) 265–274. https://doi.org/10.1016/j.fsi.2019.01.019.
58. V. da Costa, S.J. van Vliet, P. Carasi, S. Frigerio, P.A. García, D.O. Croci, M.F. Festari, M. Costa, M. Landeira, S.A. Rodríguez-Zraquia, A.J. Cagnoni, A.M. Cutine, G.A. Rabinovich, E. Osinaga, K. V. Mariño, T. Freire, The Tn antigen promotes lung tumor growth by fostering immunosuppression and angiogenesis via interaction with Macrophage Galactose-type lectin 2 (MGL2), Cancer Lett. 518 (2021) 72–81. https://doi.org/10.1016/j.canlet.2021.06.012.
59. Y. Cheng, F. Qiu, Y.C. Ye, Z.M. Guo, S.I. Tashiro, S. Onodera, T. Ikejima, Autophagy inhibits reactive oxygen species-mediated apoptosis via activating p38-nuclear factor-kappa B survival pathways in

oridonin-treated murine fibrosarcoma L929 cells, FEBS J. 276 (2009) 1291–1306. https://doi.org/10.1111/j.1742-4658.2008.06864.x.

60. A.B. Parrish, C.D. Freel, S. Kornbluth, Activation and Function, Cold Spring Harb. Perspect. Biol. 5 (2013) a008672. https://doi.org/10.1101/cshperspect.a008672.
61. L. Wang, J. Yin, X. Wang, M. Shao, F. Duan, W. Wu, P. Peng, J. Jin, Y. Tang, Y. Ruan, Y. Sun, J. Gu, C-Type Lectin-Like Receptor 2 Suppresses AKT Signaling and Invasive Activities of Gastric Cancer Cells by Blocking Expression of Phosphoinositide 3-Kinase Subunits, Gastroenterology. 150 (2016) 1183-1195.e16. https://doi.org/10.1053/j.gastro.2016.01.034.
62. G.T. Shin, H.J. Lee, J.E. Park, Growth arrest and DNA damage 45γ is required for caspase-dependent renal tubular cell apoptosis, PLoS One. 14 (2019) 1–15. https://doi.org/10.1371/journal.pone.0212818.
63. H.J. Lee, A. Nagappan, H.S. Park, G.E. Hong, S. Yumnam, S. Raha, V.V.G. Saralamma, W.S. Lee, E.H. Kim, G.S. Kim, Flavonoids isolated from Citrus platymamma induce mitochondrial-dependent apoptosis in AGS cells by modulation of the PI3K/AKT and MAPK pathways, Oncol. Rep. 34 (2015) 1517–1525. https://doi.org/10.3892/or.2015.4122.

Figures

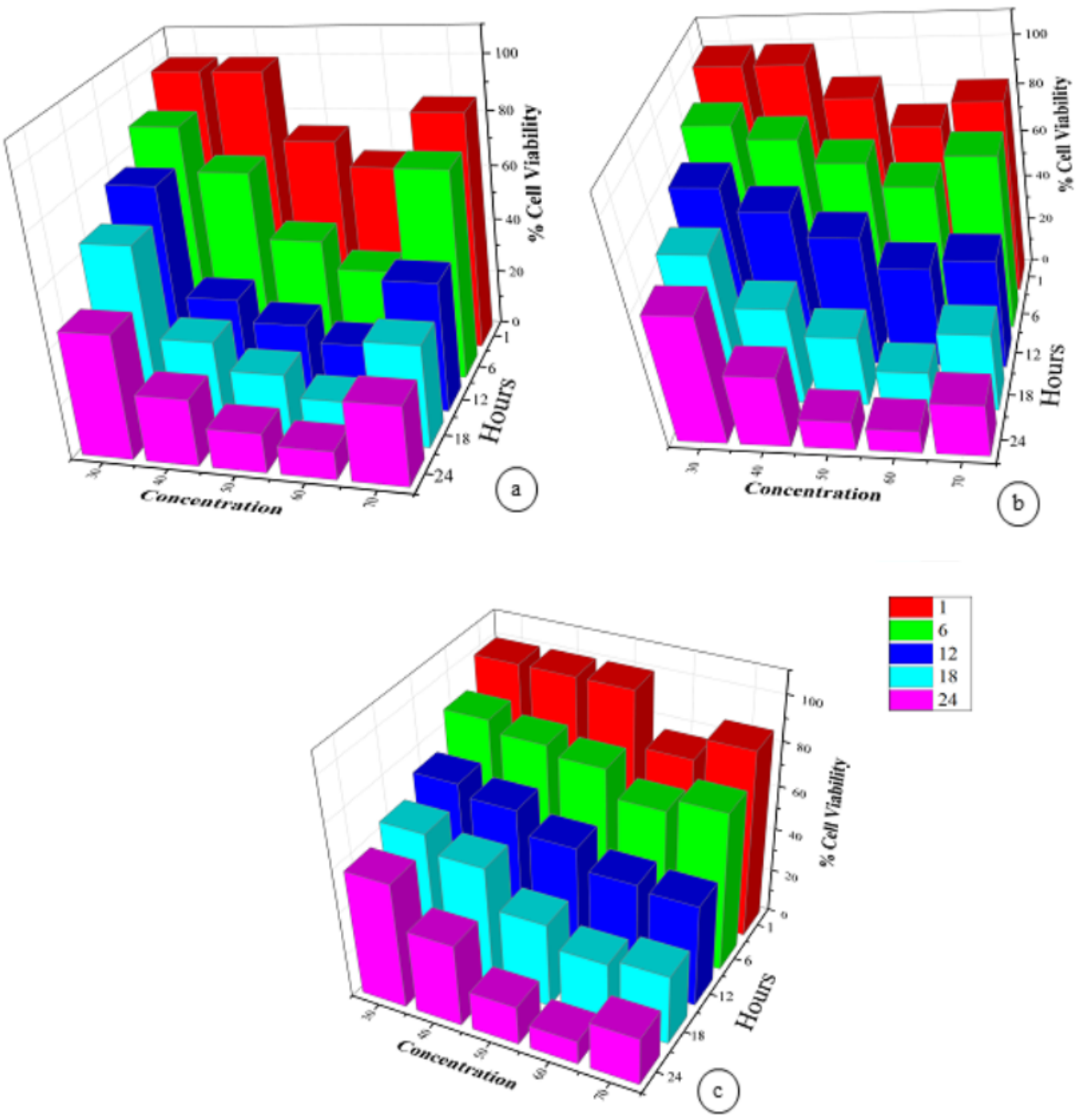

Figure 1

Effect of PFL on fungal mycelia. (a). Cell viability of *A. flavus.* (b). Cell viability of *Mucor sp.* (c).Cell viability of *A. niger.* Concentration was expressed at microgram / milliliter (µg/ml). 70 µg/ml was indicates as a standard drug.

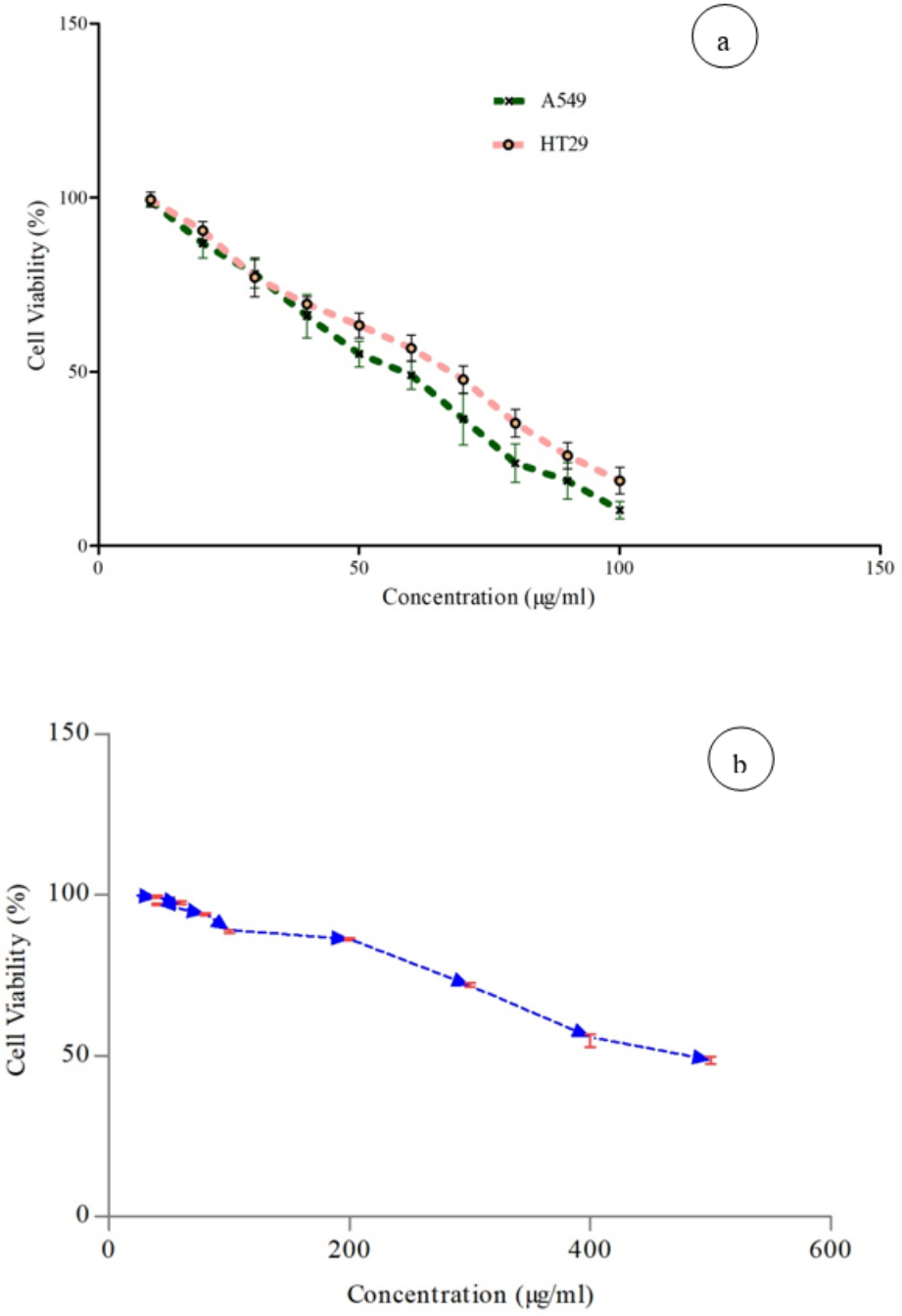

Figure 2

Cell viability of cancer cells treated with PFL-L for 24h by MTT assay. (a) Cell viability of A549 and HT29 cancer cells (b) Normal fibroblast cells with presence of PFL-L at various concentrations for 24 hours. The results are presented as the means ± SD of values obtained in three independent experiments.

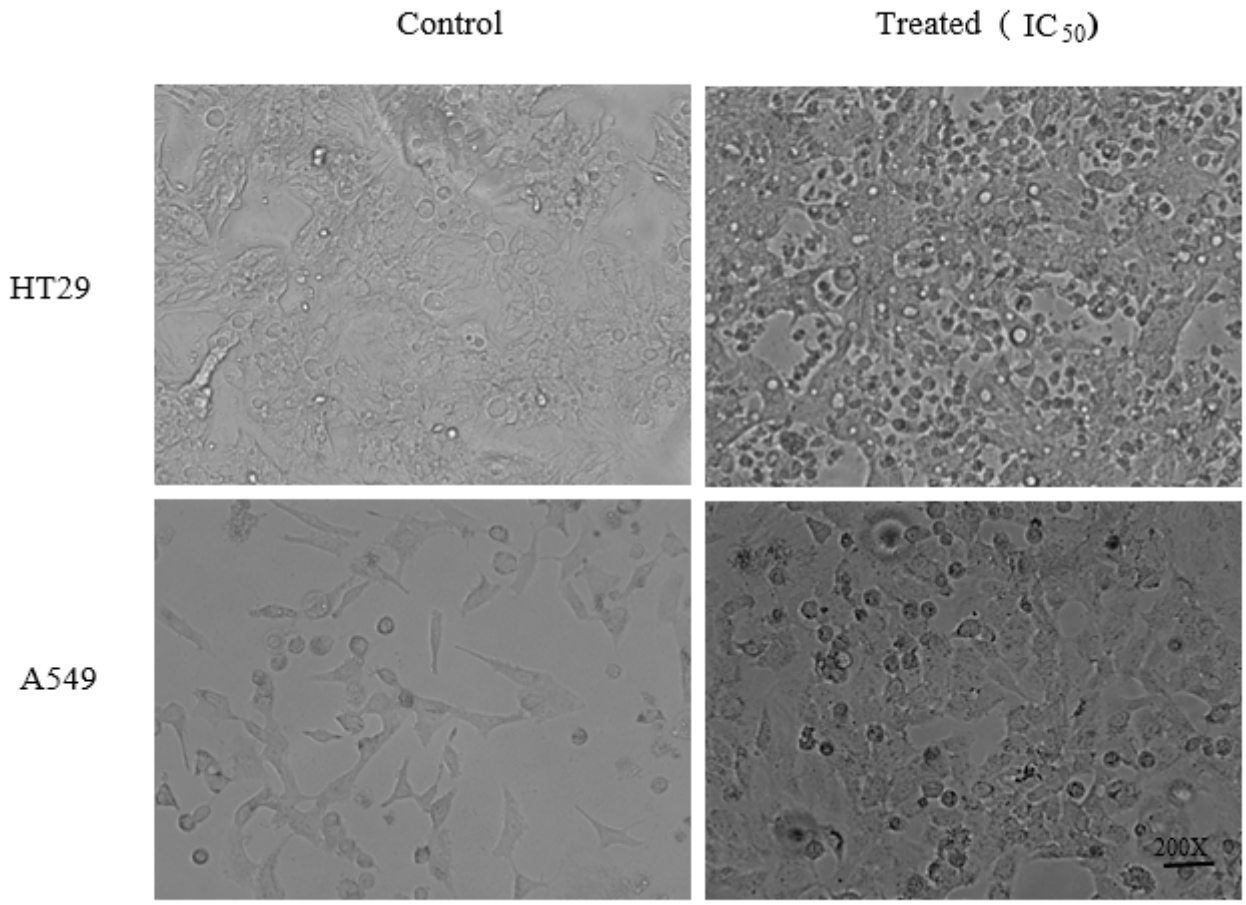

Figure 3

Cell morphological changes in A549, and HT29 cells after 24 h under a phase contrast microscope. Changes in cellular morphology were examined in absence or presence of PFL-L. PFL showed 50% inhibition at 67 µg/ml and 60 µg/ml against HT29, A549 cells respectively.

Figure 4

Morphological changes in the nuclei in absence/presence of PFL-induced apoptosis in HT29 and A549 cells detected by AO/EB and DAPI staining. (a). Acridine Orange/Ethidium Bromide (AO/EB) and DAPI after incubation (24hrs) with HT29 colon cancer cells. **(b)**. Acridine Orange/Ethidium Bromide (AO/EB) and DAPI after incubation (24hrs) on A549 cells. Viable cells showed green fluorescence. Necrotic and apoptotic cells show orange and yellow fluorescence. (Arrows indicate the following: L, live cells; A, apoptotic cells; and N, necrotic cells).

Figure 5

Single Cell Gel Electrophoresis (SCGE)/Comet Assay. Cell nucleus isolated from HT29 and A549 cells after treatment with IC_{50} concentration of respective cancer cells in alkaline nature. (a-d) Representative images of cell nuclei from HT29 and A549 cells of control/treated of PFL-L. DNA of both nuclei was stained with EtBr after separation of DNA fragments by single cell gel electrophoresis. Images were captures under a fluorescence microscopy. Scale bar 200µm. (e-f). Quantification of DNA damage of head and Tail length (in µm) indicating the extent of DNA fragmentation. Error bars represent means + s.e.m.

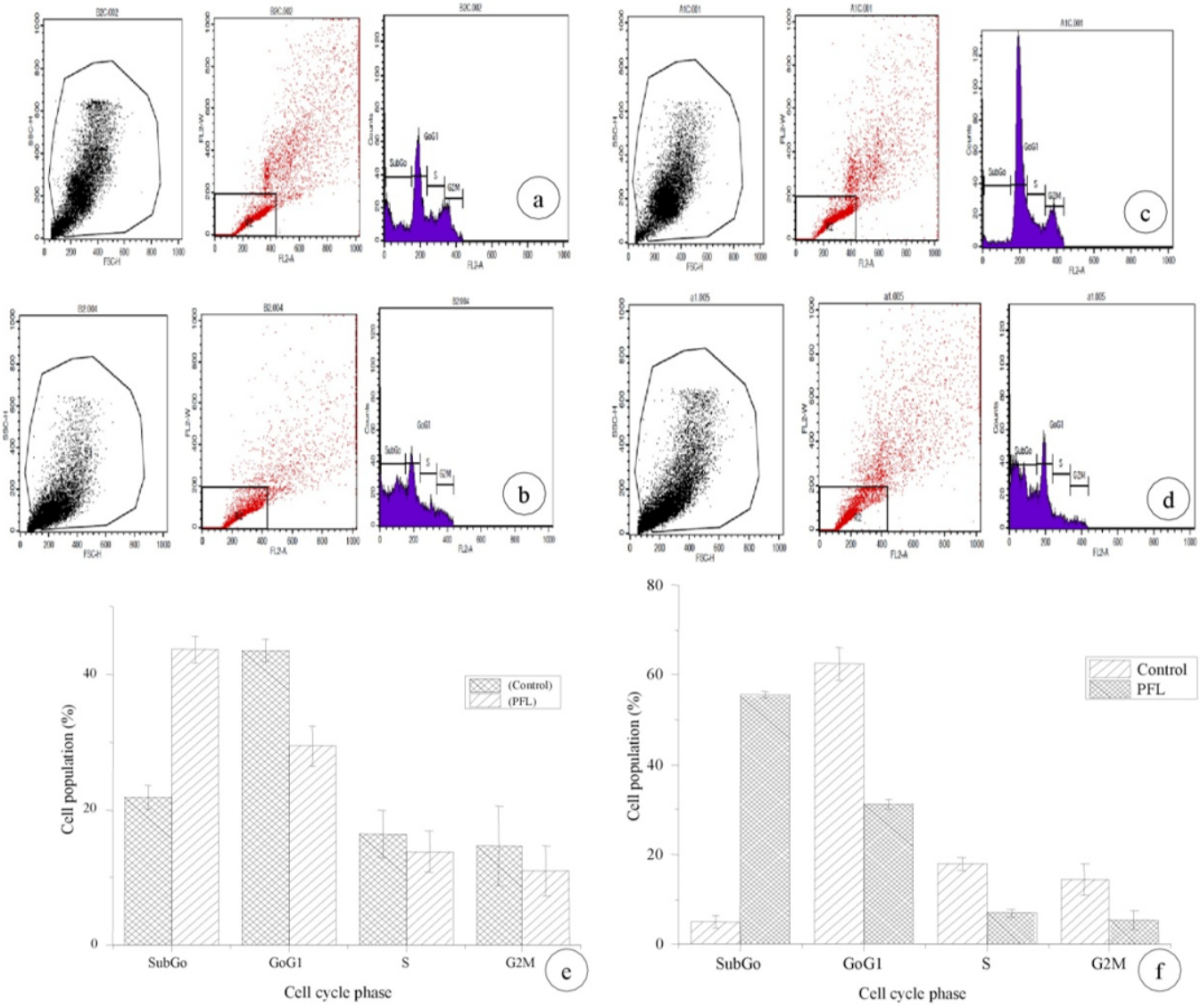

Figure 6

Flow cytometry assays measure apoptotic effect in HT29 and A549 cells treated with PFL-L at respective IC_{50} concentrations. (a). Absence of PFL-L cell cycle analysis by flow cytometry on HT29 cells. (b). Presence of PFL-L (67 µg/ml) with cell cycle analysis. (c). Absence of PFL-L cell cycle analysis by flow cytometry on A549 cells. (d). Presence of PFL-L (60 µg/ml) with cell cycle analysis. Cell cycle distribution of PI – labeled cells was analyzed by flow cytometry analysis. The peaks in the illustration correspond to the sub G0, G1/G0, S and G2/M phases of the cell cycle. (e – f). Histogram showed the percentages of cells in each phase of the cell cycle. The percentages of growth inhibition of the presence or/ absence of PFL-L with IC_{50} value on HT29 and A549 cells. The histogram was determined by flow cytometry cell cycle analysis in comparison with the different cell cycle phase. Presence of PFL-L is associated with IC_{50} both cell cycle arrest at the G0/G1 phase. Error bars represent means + s.e.m.

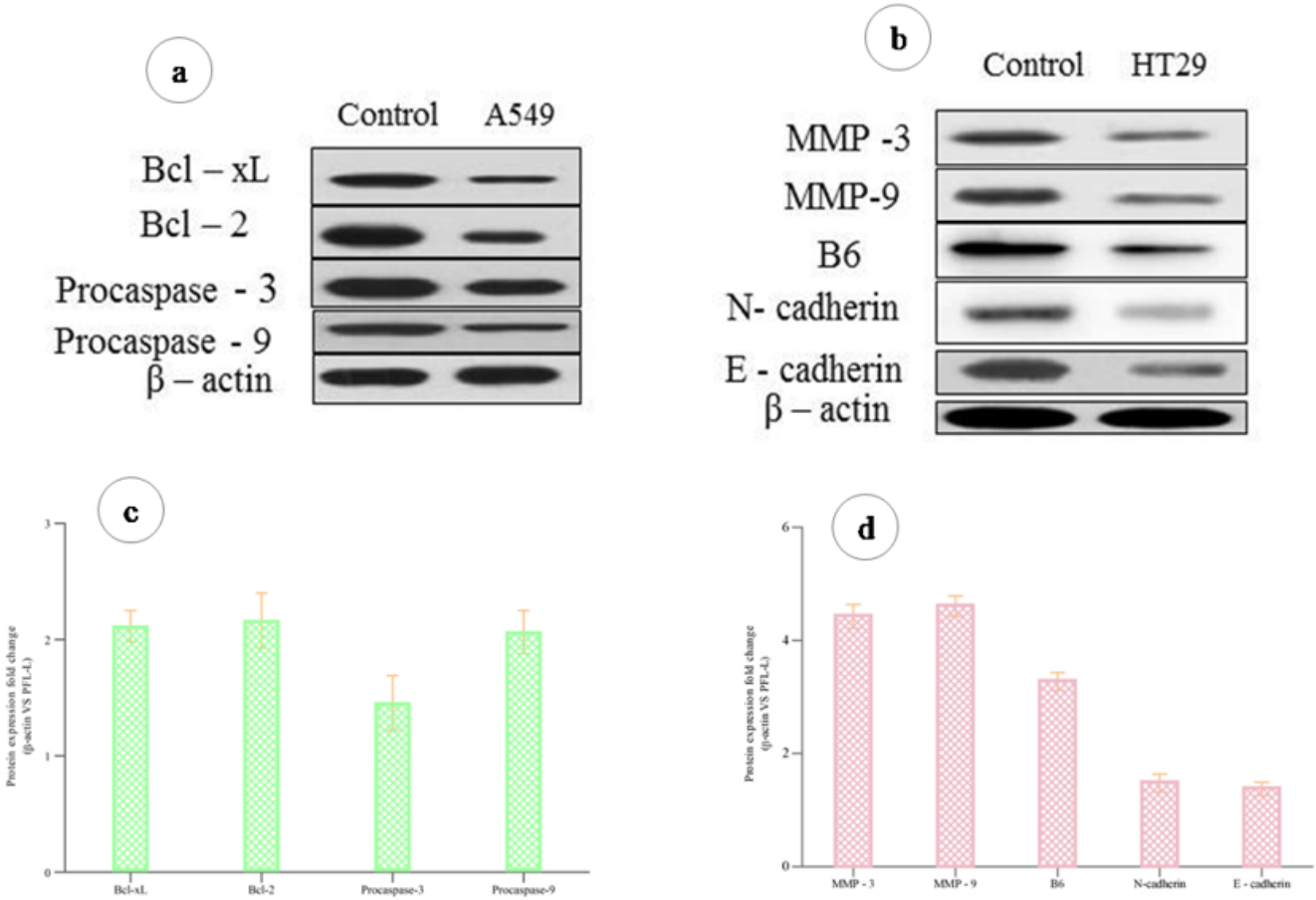

Figure 7

Western blot analysis of apoptosis related proteins after 24 hours with PFL-L. (a). A549 cells were treated with PFL-L for 24h. (b). HT29 cells were treated with PFL-L for 24h. (c). Western blot analysis of Bcl – xL, Bcl-2, Procaspase – 3, Procaspase – 9, MMP-3, MMP-9, B6, N-cadherin, and E-cadherin expression in HT29 and A549 human cancer cells. Protein levels are shown relative to the untreated control cells.

Supplementary Files

This is a list of supplementary files associated with this preprint. Click to download.

- GA.pdf